Oncology Research, Vol. 28, pp. 945–959
Printed in the USA.

0965-0407/22 $90.00 + .00
DOI: https://doi.org/10.3727/096504021X16328213967104
E-ISSN 1555-3906
www.cognizantcommunication.com

Long Noncoding RNA LAMTOR5-AS1 Interference Affects MicroRNA-506-3p/E2F6-Mediated Behavior of Non-Small Cell Lung Cancer Cells

Guojie Chen,*[1] Kai Wang,*[1] Guoshu Li,†[1] Leidong Wang,‡ Yangyang Xiao,§ and Bo Chen¶

*Department of Oncology, The First People's Hospital of Yancheng, The Fourth Affiliated Hospital of Nantong University, Jiangsu, P. R. China
†Department of Respiratory Medicine, Shanghai Tenth People's Hospital, Tongji University School of Medicine, Shanghai, P. R. China
‡Department of Pathology, Binzhou Medical University Hospital, Shandong, P. R. China
§Department of Clinical Laboratory, Binzhou Medical University Hospital, Shandong, P. R. China
¶Department of Infectious Disease, The First People's Hospital of Yancheng, The Fourth Affiliated Hospital of Nantong University, Jiangsu, P. R. China

Long noncoding RNA LAMTOR5 antisense RNA 1 (LAMTOR5-AS1) has been certified as a risk predictor and diagnostic biomarker of prostate cancer. However, the expression and exact roles of LAMTOR5-AS1 in non-small cell lung cancer (NSCLC) remain unclear. Thus, we measured LAMTOR5-AS1 expression in NSCLC and gauged its clinical value. The detailed roles and downstream working mechanism of LAMTOR5-AS1 in NSCLC were comprehensively unraveled. qRT-PCR was applied to measure gene expression. Functionally, utilizing small interfering RNA, LAMTOR5-AS1 was ablated, and the functional alterations were addressed by means of different experiments. The targeting activities between LAMTOR5-AS1 and microRNA-506-3p (miR-506-3p) and between miR-506-3p and E2F transcription factor 6 (E2F6) were confirmed by RNA immunoprecipitation and luciferase reporter assays. LAMTOR5-AS1 overexpression in NSCLC was verified in TCGA datasets and our own cohort and manifested an evident relationship with poor prognosis. Interference with LAMTOR5-AS1 led to repression of the proliferation, cloning, and metastasis abilities of NSCLC cells in vitro. We further confirmed an obvious increase in LAMTOR5-AS1-silenced NSCLC cell apoptosis. Furthermore, the absence of LAMTOR5-AS1 restricted tumor growth in vivo. Mechanistically, LAMTOR5-AS1 sponged miR-506-3p in NSCLC cells. Furthermore, E2F6, a downstream target of miR-506-3p, was under the control of LAMTOR5-AS1, which was realized by decoying miR-506-3p. Rescue experiments showed that miR-506-3p suppression or E2F6 reintroduction was capable of remitting LAMTOR5-AS1 deficiency-triggered anticarcinogenic actions in NSCLC. Our study confirmed the exact roles of LAMTOR5-AS1 for the first time and revealed that LAMTOR5-AS1 knockdown disrupts the malignancy of NSCLC by targeting the miR-506-3p/E2F6 axis. Targeting the LAMTOR5-AS1/miR-506-3p/E2F6 pathway may be instrumental for managing patients with NSCLC.

Key words: LAMTOR5-AS1; Non-small cell lung cancer (NSCLC); ceRNA regulatory theory; Targeted therapy

INTRODUCTION

Lung cancer is the most frequently occurring cancer and the leading cause of cancer-related deaths around the world[1]. According to global cancer statistics, over 2 million novel lung cancer cases occur globally, resulting in nearly 1.7 million deaths[1]. Lung cancer has two completely different histological types: non-small cell lung cancer (NSCLC) and small cell lung cancer, with the former accounting for over 85% of all lung cancer cases[2]. Although great advancements have been realized in modern diagnostic techniques over the past few decades, only approximately 20%–25% of NSCLC cases can be diagnosed at an early stage, at which point implementation of surgical excision is suitable[3]. However, when thoracalgia, chest discomfort, cough, or weight loss occurs, most patients are likely to present with late stage disease[4]. The 5-year overall survival rate for patients with

[1]These authors provided equal contribution to this work.
Address correspondence to Bo Chen, Department of Infectious Disease, The First People's Hospital of Yancheng, The Fourth Affiliated Hospital of Nantong University, 166 Yulong West Road, Yancheng, Jiangsu 224000, P. R. China. E-mail: bochen_ycph@163.com

early stage disease is approximately 14% to 49% but decreases to 5% for patients with stage IIIB/IV disease[5]. Even after conventional therapy, approximately 15% of patients with NSCLC experience a second primary cancer[6]. Furthermore, local or distant metastasis is another major obstacle in improving clinical efficiency and prognosis[7]. In this regard, determining the detailed molecular events that occur during NSCLC pathogenesis may assist in finding novel therapeutic targets.

Long noncoding RNAs (lncRNAs) are a cluster of noncoding RNA transcripts that are at least 200 nucleotides in length[8]. Previously, owing to the absence of coding regions, lncRNAs were judged to be nonfunctional or "noise" during transcription events; nevertheless, recent studies have revealed their significant functions in a wide variety of aggressive processes[9–11]. lncRNAs perform critical regulatory actions in the process of NSCLC oncogenesis and progression[12,13]. lncRNAs have tumor-inhibiting or tumor-promoting capabilities and are implicated in the control of many aggressive tumor properties[14].

MicroRNAs (miRNAs) refer to a group of evolutionarily conserved and noncoding short RNA transcripts consisting of 17–22 nucleotides[15]. They have been certified as essential epigenetic factors that regulate gene expression via interacting with the 3'-untranslated region of their downstream target genes, ultimately triggering translation suppression or mRNA degradation[16]. Aberrant miRNA expression is widely observed in NSCLC occurrence and development and contributes to an extensive range of malignant behaviors[17]. Recently, an increasing number of studies have highlighted that the competing endogenous RNA (ceRNA) regulatory network has a role in NSCLC[18–20]. According to this theory, lncRNAs act as "miRNA sponges" or ceRNAs and thus control downstream target genes.

LAMTOR5-AS1 has been identified as a risk prediction and diagnostic biomarker of prostate cancer[21]. Nonetheless, the exact functions of LAMTOR5-AS1 in NSCLC remain poorly understood and demand further investigation. In view of this, in our current study, we aimed to probe the LAMTOR5-AS1 level in NSCLC and assess its clinical significance. Furthermore, we comprehensively unraveled the detailed roles and downstream working mechanism of LAMTOR5-AS1 in NSCLC.

MATERIALS AND METHODS

Clinical Specimens

The present study received approval from the Ethics Committee of The First People's Hospital of Yancheng and was implemented in accordance with the Declaration of Helsinki. We collected NSCLC tissues and paired adjacent normal tissues from 49 patients in our hospital. All patients offered written informed consent before tissue collection. The exclusion criteria included patients who had received radiochemotherapy or other anticancer treatments, patients with other cancer types, and patients who refused to take part in the research.

Cell Culture

The NSCLC cell lines NCI-H460 (H460) and NCI-H522 [H522; American Type Culture Collection (ATCC), Manassas, VA, USA] were grown in F-12K medium (Gibco; Thermo Fisher Scientific Inc., Waltham, MA, USA). The NSCLC cell lines A549 (ATCC) and NCI-H1299 (H1299; National Collection of Authenticated Cell cultures, Shanghai, China) were cultured in RPMI-1640 medium. Minimum essential medium was applied for culture of the NSCLC cell line SK-MES-1 (ATCC). BEAS-2B (ATCC), an immortalized human bronchial epithelial mesothelial cell line, was maintained in bronchial epithelial cell growth medium (Lonza, Walkersville, MD, USA). Meanwhile, 10% fetal bovine serum (FBS; Gibco) was used in the cultures of all of the above cell lines, which were cultivated at 37°C in a humidified atmosphere with 5% CO_2.

Transfection

Shanghai GenePharma Co. Ltd. (Shanghai, China) chemically synthesized three specific small interfering (si)RNAs targeting LAMTOR5-AS1 (si-LAMTOR5-AS1s) and a scramble control siRNA (si-NC). The si-LAMTOR5-AS1#1 sequence was 5′-TTGTAAAA TTGAAATATTTGAAT-3′, the si-LAMTOR5-AS1#2 sequence was 5′-TACCAAAAAATAAAAATATGAAC-3′, the si-LAMTOR5-AS1#3 sequence was 5′-GGCA TACTTAGTTTTACATTTTT-3′, and the si-NC sequence was 5′-CACGATAAGACAATGTATTT-3′. Increases and decreases in miR-506-3p were achieved through an miR-506-3p mimic and an miR-506-3p inhibitor, respectively (Shanghai GenePharma Co. Ltd.). An miRNA mimic control (miR-NC) and a negative control (NC) inhibitor served as the controls. GenScript Biotech Corp. (Nanjing, China) prepared full-length E2F6 and then ligated it into a pcDNA™ 3.1 vector, consequently yielding pcDNA3.1-E2F6. When the cell density reached approximately 60%–70% confluence, cell transfection was conducted applying Lipofectamine® 2000 (Invitrogen, Carlsbad, CA, USA).

Quantitative Real-Time Polymerase Chain Reaction (qRT-PCR)

TRIzol (Beyotime, Shanghai, China) was adopted for total RNA abstraction. The concentration and quality of total RNA were tested with a NanoDrop® 2000 spectrophotometer (Thermo Fisher Scientific Inc.). For detection of LAMTOR5-AS1 and E2F6, we reverse transcribed total RNA into first-strand complementary DNA with a

PrimeScript™ RT reagent kit (Takara, Dalian, China). Next, PCR amplification was carried out by means of TB Green® Premix Ex Taq™ II (Takara). To determine the miR-506-3p level, we conducted reverse transcription and quantitative PCR utilizing an miRcute miRNA First-Strand cDNA Synthesis Kit and an miRcute miRNA qPCR Detection Kit SYBR Green (Tiangen Biotech, Beijing, China), respectively. The $2^{-\Delta\Delta Cq}$ method[22] was employed for quantification of the expression of all genes.

Cell Counting Kit-8 (CCK-8) and Colony Formation Assays

We collected the transfected cells and resuspended them in complete culture medium at a concentration of 3×10^4 cells/ml. Each well from 96-well plates was covered with 100 µl of cell suspension. At the set time points after cell inoculation, the cells were probed with 10 µl of CCK-8 solution (Beyotime) at 37°C for 2 h. The absorbance was read at 450-nm wavelength using a microplate reader (Bio-Rad, Hercules, CA, USA).

Transfected cells were collected, and a cell suspension was prepared in the same manner as described above. Cells were spread evenly in six-well plates at a density of 1,000 cells/well. We allowed the cells to form colonies at 37°C for 14 days. Finally, the colonies were rinsed with phosphate-buffered saline (PBS), fixed using 100% methanol, and stained with 0.05% crystal violet. The colonies were counted under a microscope (Nikon, Tokyo, Japan).

Transwell Experiments

To detect migration ability, 1×10^5 cells were added to the upper compartments of the Transwell chambers (8-µm pores; Corning Costar, Cambridge, MA, USA) containing 100 µl of FBS-free medium. Twenty percent FBS-supplemented culture medium was placed into the lower chambers. We incubated cells at 37°C for 1 day and then used a cotton bud to manually wipe away the nonmigrated cells. The migrated cells were treated with 100% methanol for fixation and 0.05% crystal violet for coloration. Next, we employed an inverted light microscope to take photos and count the migrated cells. To assess invasion capacity, the top layer surface of the membrane was coated with Matrigel (BD Bioscience, San Jose, CA, USA) in advance, and the subsequent experimental steps were the same as those described above.

Flow Cytometry Analysis

Transfected cells were harvested via treatment with 0.25% EDTA-free trypsin, washed with PBS, and centrifuged to remove the supernatant fluid. Evaluation of cell apoptosis was achieved with the help of an Annexin-V–FITC/PI Apoptosis Kit (KeyGEN, Nanjing, China). In total, 500 µl of binding buffer was utilized to resuspend the transfected cells, which were then mixed with 5 µl of annexin V–fluorescein isothiocyanate (FITC) and 5 µl of propidium iodide. After cultivation at room temperature without light, the proportion of apoptotic cells was measured with a FACScan flow cytometer (BD Bioscience).

Tumor Xenograft Experiment

The experiments involving animals were implemented with approval from the Animal Ethics Committee of The First People's Hospital of Yancheng and followed the National Institutes of Health *Guidelines for the Care and Use of Laboratory Animals*. Shanghai GenePharma Co. Ltd. synthesized short-hairpin RNA (shRNA) targeting LAMTOR5-AS1 (sh-LAMTOR5-AS1) and scramble control shRNA (sh-NC) and inserted these constructs into a lentiviral vector, producing recombinant lentiviral vectors. The sh-LAMTOR5-AS1 sequence was 5′-CCGGT ACCAAAAAATAAAAATATGAACCTCGAGGTTCA TATTTTTATTTTTTGGTATTTTTG-3′, and the sh-NC sequence was 5′-CCGGCACGATAAGACAATGTATT TCTCGAGAAATACATTGTCTTATCGTGTTTTTG-3′. After transfection of 293T cells with the appropriate lentiviral vector along with psPAX2 and pMD2.G, the lentiviral particles were harvested after 48 h of culture at 37°C. For acquisition of a stable LAMTOR5-AS1-knockdown cell line, A549 cells were cultivated with culture medium containing lentiviral particles and selected with puromycin.

Male BALB/c nude mice, aged 4–6 weeks, were acquired from Vital River Laboratory (Beijing, China) and maintained under specific pathogen-free conditions at 25°C and 50% humidity with a 10:14 light/dark cycle and ad libitum access to food and water. A total of 1×10^6 stable LAMTOR5-AS1-knockdown A549 cells were resuspended in 100 µl of PBS and subcutaneously injected into the flank of mice. One week after cell injection, tumor size was recorded every 4 days and used to determine tumor volume based on the following equation: volume = $0.5 \times \text{length} \times \text{width}^2$. At 31 days after cell injection, all mice were euthanized by cervical dislocation, and we excised the tumor xenografts for tumor weight assessment and further immunohistochemistry analyses.

Fluorescence In Situ Hybridization

We analyzed the in situ localization of LAMTOR5-AS1 in NSCLC cells using a Fluorescent In Situ Hybridization (FISH) Kit (Guangzhou RiboBio Co. Ltd., Science City, Guangzhou, China). Briefly, we rinsed NSCLC cells twice with PBS, fixed them with 4% paraformaldehyde, and treated them with probes specifically targeting LAMTOR5-AS1 (Guangzhou RiboBio Co. Ltd.) at 37°C overnight without light. Next, DNA staining was done using Hoechst solution. Finally, imaging was implemented under a confocal laser scanning microscope (Leica, Solms, Germany).

Nuclear/Cytoplasmic Fractionation Assay

We collected cells in the logarithmic growth phase and subjected these cells to a PARIS™ Kit (Thermo Fisher Scientific Inc.) to obtain nuclear/cytoplasmic fractions. After RNA extraction, qRT-PCR was carried out to determine the subcellular localization of LAMTOR5-AS1.

Bioinformatics Prediction and Luciferase Reporter Assay

The putative targets of LAMTOR5-AS1 were predicted with starBase 3.0 (http://starbase.sysu.edu.cn/). The prediction of the miR-506-3p downstream targets was conducted using two algorithms, including miRDB (http://mirdb.org/) and TargetScan (http://www.targetscan.org/).

Partial fragments of LAMTOR5-AS1 carrying wild-type (WT) or mutant (MT) miR-506-3p-binding sites were synthesized by Shanghai GenePharma Co. Ltd. and cloned into a psiCHECK2 vector (Promega, Madison, WI, USA). The generated luciferase reporter plasmids were labeled WT-LAMTOR5-AS1 and MUT-LAMTOR5-AS1. In a similar manner, WT-E2F6 and MUT-E2F6 reporter plasmids were produced. For the reporter assay, NSCLC cells were transiently transfected with the indicated plasmids alongside miR-506-3p mimic or miR-NC. Two days after transfection, the luciferase activity was examined utilizing a Dual-Luciferase Reporter Assay System (Promega).

RNA Immunoprecipitation (RIP)

By utilizing a Magna RIP RNA Binding Protein Immunoprecipitation Kit (Merck Millipore, Darmstadt, Germany), we examined the interaction among LAMTOR5-AS1, miR-506-3p, and E2F6. In brief, whole NSCLC cell lysates were obtained by treatment of cells with complete RIP lysis buffer and probed overnight at 4°C with RIP buffer supplemented with magnetic beads containing anti-Argonaute2 (Ago2) antibody or IgG control (Millipore). Then the magnetic beads were harvested and rinsed using RIP washing buffer, followed by treatment with Proteinase K buffer. The target immunoprecipitated RNA was extracted and detected via qRT-PCR.

Western Blot Analysis

We isolated total protein using RIP assay (RIPA) lysis buffer containing phenylmethanesulfonyl fluoride (Beyotime). After quantification with a BCA Protein Assay Kit (Beyotime), the same amounts of protein were loaded and subjected to separation in 10% sodium dodecyl sulfate-polyacrylamide gel electrophoresis (SDS-PAGE), after which the proteins were transferred onto a polyvinylidene difluoride (PVDF) membrane. Subsequently, the membranes were immersed in 5% nonfat dry milk at room temperature for 2 h and incubated overnight at 4°C with primary antibodies targeting E2F6 (Cat. No. ab11952) or GAPDH (Cat. No. ab8245; both from Abcam, Cambridge, UK). Next, a further 2-h incubation at room temperature was conducted with a horseradish peroxidase (HRP)-conjugated secondary antibody (Cat. No. ab205719; Abcam). Finally, Pierce™ ECL Western Blotting Substrate (Thermo Fisher Scientific Inc.) was adopted for target signal visualization.

Statistical Analysis

All data were obtained from three independent experiments and are expressed as the mean ± standard deviation. Survival analysis was implemented utilizing the Kaplan–Meier method and a log rank test. The evaluation of differences between two groups was achieved using paired or unpaired Student's *t*-tests. One-way analysis of variance (ANOVA) followed by Tukey's test was employed to assess differences between multiple groups. Gene expression correlation was tested using Pearson's correlation coefficient. A value of $p < 0.05$ was considered to indicate a statistically significant difference.

RESULTS

LAMTOR5-AS1 Depletion Induces Inhibition of Malignant Characteristics in NSCLC

The expression status of LAMTOR5-AS1 in NSCLC was discovered using The Cancer Genome Atlas (TCGA) database (https://portal.gdc.cancer.gov/). Compared with normal tissues, LAMTOR5-AS1 was overexpressed in both lung adenocarcinoma (LUAD) and lung squamous cell carcinoma (LUSC) (Fig. 1A). Next, we measured LAMTOR5-AS1 expression in our own cohort. LAMTOR5-AS1 was observably overexpressed in NSCLC tissues compared to adjacent normal tissues (Fig. 1B). In contrast to BEAS-2B cells, the tested NSCLC cell lines manifested higher LAMTOR5-AS1 levels (Fig. 1C). Based on the median value of LAMTOR5-AS1 in NSCLC tumor tissues, all patients with NSCLC were divided into either the low LAMTOR5-AS1 group ($n = 24$) or the high LAMTOR5-AS1 group ($n = 25$). NSCLC cases with high LAMTOR5-AS1 levels presented evidently shorter overall survival than cases with low LAMTOR5-AS1 levels (Fig. 1D).

The high level of LAMTOR5-AS1 expression in NSCLC and its correlation with overall survival compelled us to uncover its role in NSCLC progression. A549 and SK-MES-1 cells manifested the highest LAMTOR5-AS1 level among the five NSCLC cell lines; therefore, they were applied in subsequent functional experiments. Through siRNAs, LAMTOR5-AS1 was depleted in A549 and SK-MES-1 cells (Fig. 2A). si-LAMTOR5-AS1#1 and si-LAMTOR5-AS1#2 were applied for further investigation because their knockdown efficiency was higher than that of si-LAMTOR5-AS1#3. Interference with LAMTOR5-AS1 expression impeded the proliferation (Fig. 2B) and cloning ability (Fig. 2C) of NSCLC cells. In addition, flow

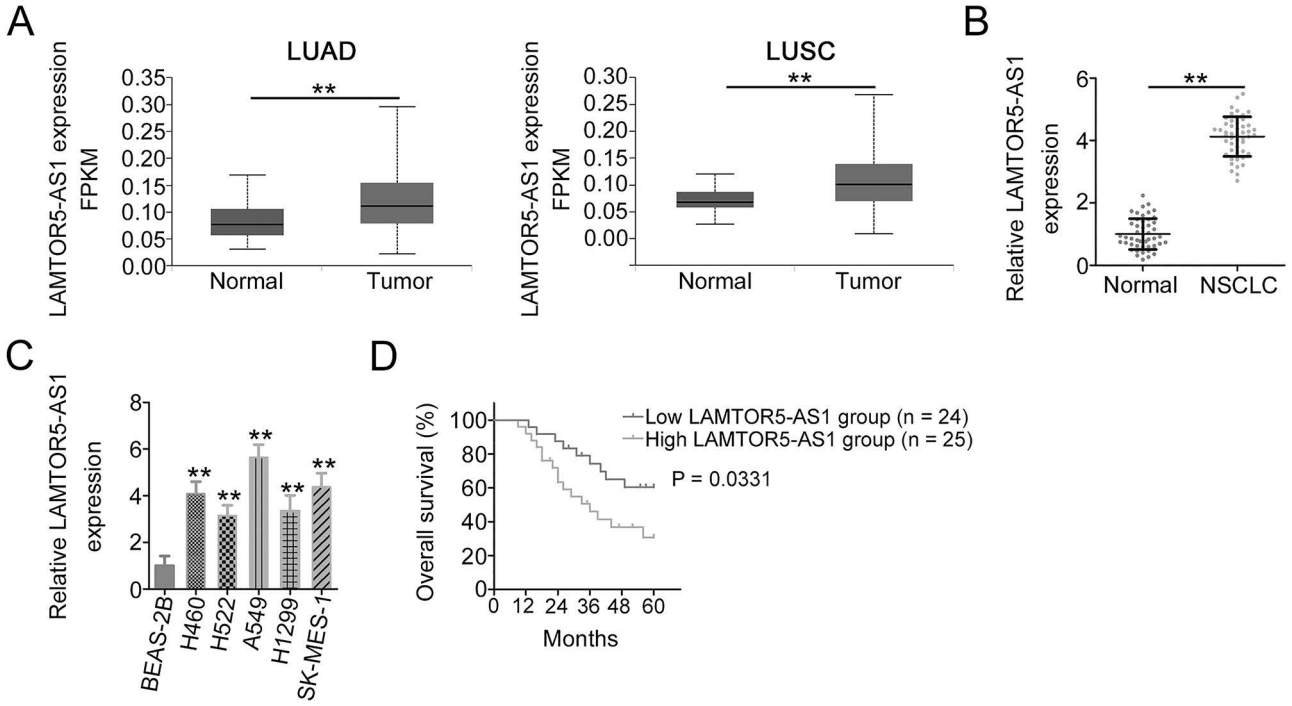

Figure 1. LAMTOR5-AS1 is overexpressed in non-small cell lung cancer (NSCLC). (A) The fragments per kilobase per million (FPKM) expression values of LAMTOR5-AS in lung adenocarcinoma (LUAD) and lung squamous cell carcinoma (LUSC) were determined using The Cancer Genome Atlas (TCGA). (B) Assessment of LAMTOR5-AS1 levels in NSCLC tissues was performed via quantitative real-time polymerase chain reaction (qRT-PCR). (C) qRT-PCR was adopted to measure LAMTOR5-AS1 levels in NSCLC cell lines. (D) Kaplan–Meier curves revealed the prognosis of NSCLC cases with high or low LAMTOR5-AS1 expression. $^{**}p < 0.01$.

cytometry analysis was implemented, verifying that cell apoptosis was increased after knockdown of LAMTOR5-AS1 (Fig. 2D). Furthermore, depletion of LAMTOR5-AS1 led to a clear decrease in NSCLC cell migration and invasion (Fig. 3A and B). Overall, LAMTOR5-AS1 knockdown disrupted the malignancy of NSCLC.

LAMTOR5-AS1 Competitively Binds to miR-506-3p in NSCLC

Based on the results of the nuclear/cytoplasmic fractionation experiment and fluorescence in situ hybridization, LAMTOR5-AS1 was confirmed to be mainly expressed in the cell cytoplasm (Fig. 4A and B), indicating that LAMTOR5-AS1 may perform its cancer-promoting actions by acting as a molecular sponge or ceRNA. As predicted by the starBase 3.0 tool, 46 miRNAs were identified as possible downstream targets of LAMTOR5-AS1. We then analyzed the expression profile of the 46 candidates in NSCLC by analyzing TCGA datasets. miR-506-3p was downregulated in both LUAD and LUSC (Fig. 4C) and therefore was selected for subsequent studies. For further verification, qRT-PCR was implemented to measure the expression of miR-506-3p in LAMTOR5-AS1-silenced NSCLC cells. Transfection with si-LAMTOR5-AS1 increased the level of miR-506-3p in NSCLC cells (Fig. 4D).

Later, the direct binding between LAMTOR5-AS1 and miR-506-3p (Fig. 4E) was explored using a luciferase reporter assay. The luciferase activity of WT-LAMTOR5-AS1 was diminished upon miR-506-3p overexpression, but when the binding sequences were mutated, the miR-506-3p mimic was unable to alter the luciferase activity (Fig. 4F). Ago2 is a key element of the RNA-induced silencing complex and can directly trigger the degradation of targets through its catalytic activity in gene silencing processes guided by miRNAs. In a RIPA, miR-506-3p and LAMTOR5-AS1 were evidently enriched in Ago2-containing beads compared with the IgG group (Fig. 4G). In addition, the miR-506-3p level was reduced in NSCLC tissues (Fig. 4H) and manifested an inverse relationship with LAMTOR5-AS1 expression (Fig. 4I). Undoubtedly, LAMTOR5-AS1 operated as a miR-506-3p sponge in NSCLC.

LAMTOR5-AS1 Positively Regulates E2F6 Expression in NSCLC by Sequestering miR-506-3p

To illuminate the role of miR-506-3p in NSCLC, we overexpressed miR-506-3p in NSCLC cells using a

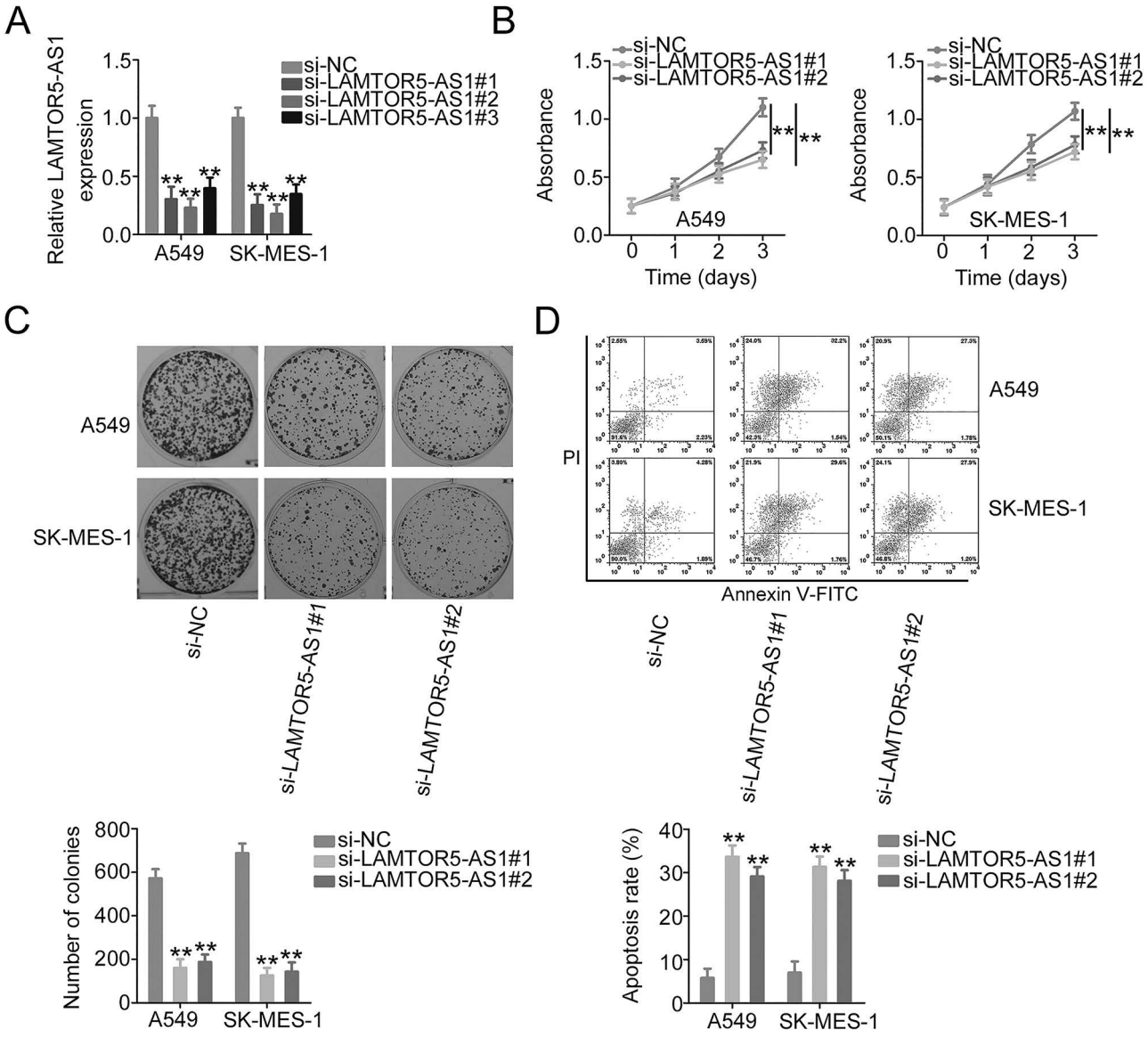

Figure 2. LAMTOR5-AS1 downregulation impairs the malignant progression of NSCLC. (A) qRT-PCR confirmed the silencing efficiency of siRNAs targeting LAMTOR5-AS1. (B, C) Cell Counting Kit-8 (CCK-8) and colony formation assays illustrated the growth of NSCLC cells after LAMTOR5-AS1 depletion. (D) The proportion of apoptotic LAMTOR5-AS1-deficient NSCLC cells was tested via flow cytometry analysis. $^{**}p < 0.01$.

miR-506-3p mimic (Fig. 5A). Through functional experiments, exogenous miR-506-3p was found to restrict NSCLC cell proliferation (Fig. 5B and C), trigger cell apoptosis accumulation (Fig. 5D), and hinder cell motility (Fig. 5E and F). To identify potential targets of miR-506-3p, bioinformatics prediction was conducted and revealed that E2F6, a well-known oncogene in various human cancer types, may be a possible candidate target of miR-506-3p (Fig. 6A). miR-506-3p upregulation observably downregulated E2F6 in NSCLC cells (Fig. 6B and C). Moreover, E2F6 overexpression in NSCLC (Fig. 6D) presented a clear negative correlation with miR-506-3p expression (Fig. 6E). Moreover, the miR-506-3p mimic weakened the luciferase activity of WT-E2F6, whereas the activity caused by MUT-E2F6 remained largely unchanged despite the same cotransfection status (Fig. 6F).

We next attempted to examine whether LAMTOR5-AS1 is implicated in modulating E2F6 expression by acting as an miR-506-3p sponge. Loss of LAMTOR5-AS1 resulted in a decrease in E2F6 expression (Fig. 6G and H), which was abrogated by cotransfection with the miR-506-3p inhibitor (Fig. 6I and J). Additionally, a positive expression relationship was affirmed between LAMTOR5-AS1 and E2F6 in NSCLC tissues (Fig. 6K).

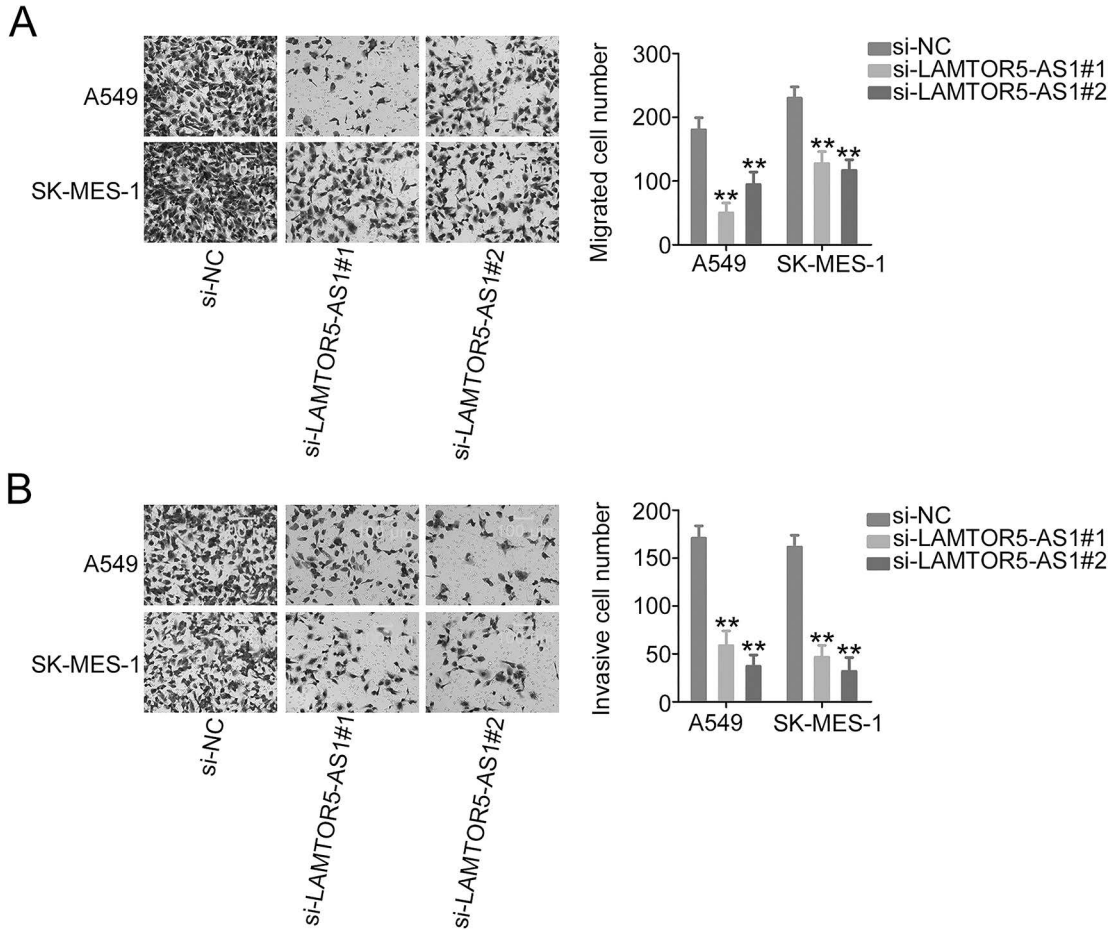

Figure 3. LAMTOR5-AS1 knockdown decreases the migration and invasion of NSCLC. (A, B) Transwell experiments revealed the motility of NSCLC cells after transfection with siRNA to induce LAMTOR5-AS1 downregulation. $^{**}p < 0.01$.

Finally, as evidenced by the RIP results, the enrichment of LAMTOR5-AS1, miR-506-3p, and E2F6 was confirmed in Ago2-precipitated products (Fig. 6L), indicating the coexistence of the three RNAs in the RNA-induced silencing complex. Thus, LAMTOR5-AS1 positively controlled E2F6 expression in NSCLC by decoying miR-506-3p.

LAMTOR5-AS1 Ablation Hinders NSCLC Cell Behaviors by Increasing the Output of the miR-506-3p/E2F6 Axis

Rescue experiments were carried out to determine whether the miR-506-3p/E2F6 axis is required for the anticarcinogenic actions of si-LAMTOR5-AS1 in NSCLC cells. First, the knockdown efficiency of the miR-506-3p inhibitor was verified via qRT-PCR (Fig. 7A). Treatment with the miR-506-3p inhibitor reversed the decrease in NSCLC cell proliferation and colony formation mediated by LAMTOR5-AS1 downregulation (Fig. 7B and C). Furthermore, downregulation of LAMTOR5-AS1 promoted cell apoptosis, which was neutralized after miR-506-3p depletion (Fig. 7D). Additionally, the impaired migratory and invasive properties of LAMTOR5-AS1-deficient NSCLC cells were restored by miR-506-3p inhibition (Fig. 7E).

In addition, Western blotting verified the overexpression efficiency of pcDNA3.1-E2F6 in NSCLC cells (Fig. 8A). Reintroduction of E2F6 reversed the si-LAMTOR5-AS1-mediated effects on NSCLC cell proliferation and cloning abilities (Fig. 8B and C) as well as on cell apoptosis (Fig. 8D). Additionally, the decreased migration and invasion induced by si-LAMTOR5-AS1 were recovered by E2F6 restoration (Fig. 8E). Collectively, the results indicate that the absence of LAMTOR5-AS1 repressed the malignant progression of NSCLC cells via control of the miR-506-3p/E2F6 axis.

LAMTOR5-AS1 Downregulation Impedes Tumor Growth In Vivo

Finally, a tumor xenograft experiment was carried out to characterize the effect of LAMTOR5-AS1 on tumor growth in vivo. At 31 days after cell injection,

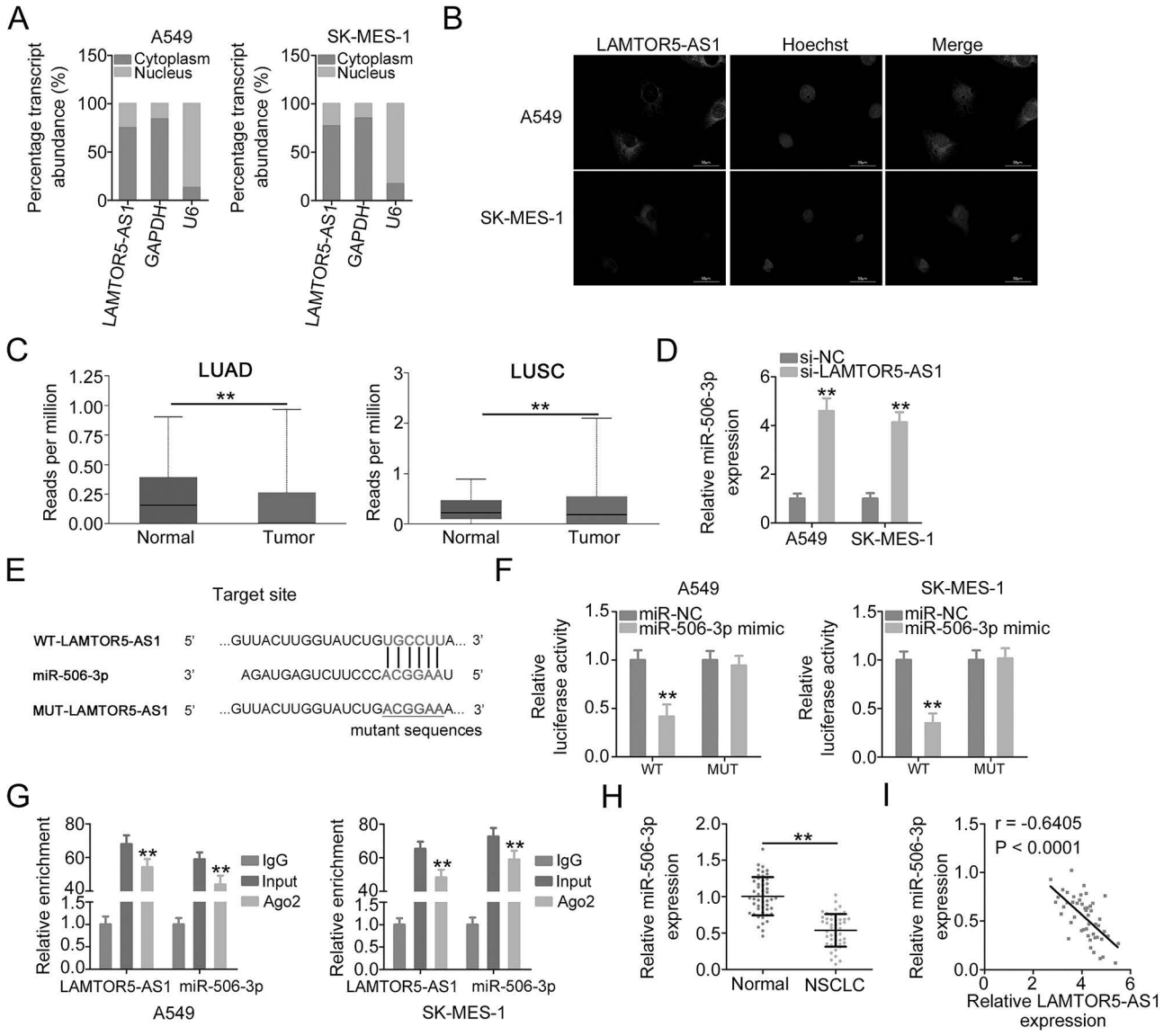

Figure 4. LAMTOR5-AS1 acts as an miR-506-3p sponge in NSCLC. (A, B) Localization of LAMTOR5-AS1 in A549 and SK-MES-1 cells. (C) miR-506-3p expression in LUAD and LUSC was examined using TCGA databases. (D) After LAMTOR5-AS1 ablation, the expression of miR-506-3p was examined via qRT-PCR. (E) Wild-type (WT) and mutant (MUT) binding sequences of miR-506-3p within LAMTOR5-AS1 sequences. (F) Luciferase activity was evaluated in miR-506-3p-overexpressing NSCLC cells after transfection with WT-LAMTOR5-AS1 or MUT-LAMTOR5-AS1. (G) The enrichment of LAMTOR5-AS1 and miR-506-3p by Ago2 antibody was confirmed with a RNA immunoprecipitation (RIP) assay. (H) qRT-PCR was applied to measure miR-506-3p expression in NSCLC tissues. (I) Pearson's correlation analysis illustrated the relation between LAMTOR5-AS1 and miR-506-3p in NSCLC tissues. $^{**}p < 0.01$.

tumor xenografts were excised (Fig. 9A). Tumor xenografts from the sh-LAMTOR5-AS1 group featured slower growth (Fig. 9B) and a lower weight (Fig. 9C) than those from the sh-NC group. Furthermore, compared with the sh-NC group, LAMTOR5-AS1 was downregulated (Fig. 9D), whereas miR-506-3p was overexpressed (Fig. 9E) in sh-LAMTOR5-AS1-injected tumors. Additionally, E2F6 protein was evidently downregulated in xenografts from the sh-LAMTOR5-AS1 group (Fig. 9F). Immunohistochemistry analysis showed that the levels of E2F6 and the proliferation marker Ki-67 were reduced, while those of the apoptotic marker cleaved caspase-3 were increased in LAMTOR5-AS1-depleted tumors (Fig. 9G). In short, LAMTOR5-AS1 downregulation led to in vivo tumor growth suppression.

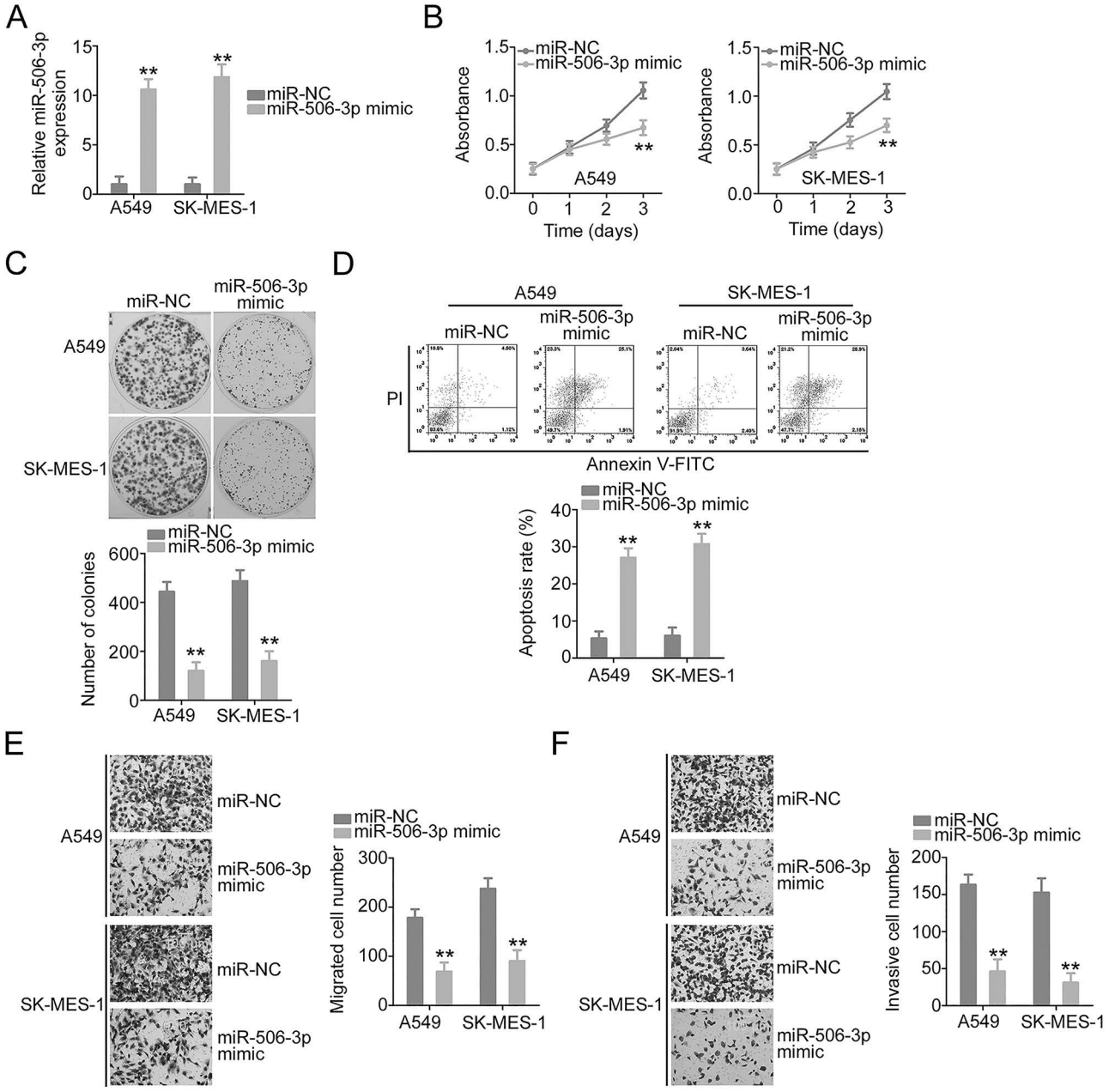

Figure 5. miR-506-3p reintroduction attenuates the malignant behaviors of NSCLC cells. (A) The transfection efficiency of miR-506-3p mimic in NSCLC. (B, C) miR-506-3p-overexpressing NSCLC cell proliferation and colony formation. (D) Apoptosis of NSCLC cells transfected with the miR-506-3p mimic was examined. (E, F) The migratory and invasive properties of miR-506-3p-overexpressing NSCLC cells were determined via Transwell experiments. $^{**}p < 0.01$.

DISCUSSION

Numerous studies have authenticated the multifaceted functions of lncRNAs in the onset and progression of NSCLC[23–25]. With the great advancements made in next-generation sequencing technology, a considerable number of lncRNAs have been found to induce dysregulation in NSCLC[26]; however, the exact functions of the vast majority of lncRNAs in NSCLC await further exploration. Thus, identifying lncRNAs that contribute to NSCLC pathogenesis has become an area of interest for many researchers and would be of instrumental significance for managing NSCLC patients. In this study, we measured LAMTOR5-AS1 expression in NSCLC and gauged its clinical value. Furthermore, LAMTOR5-AS1

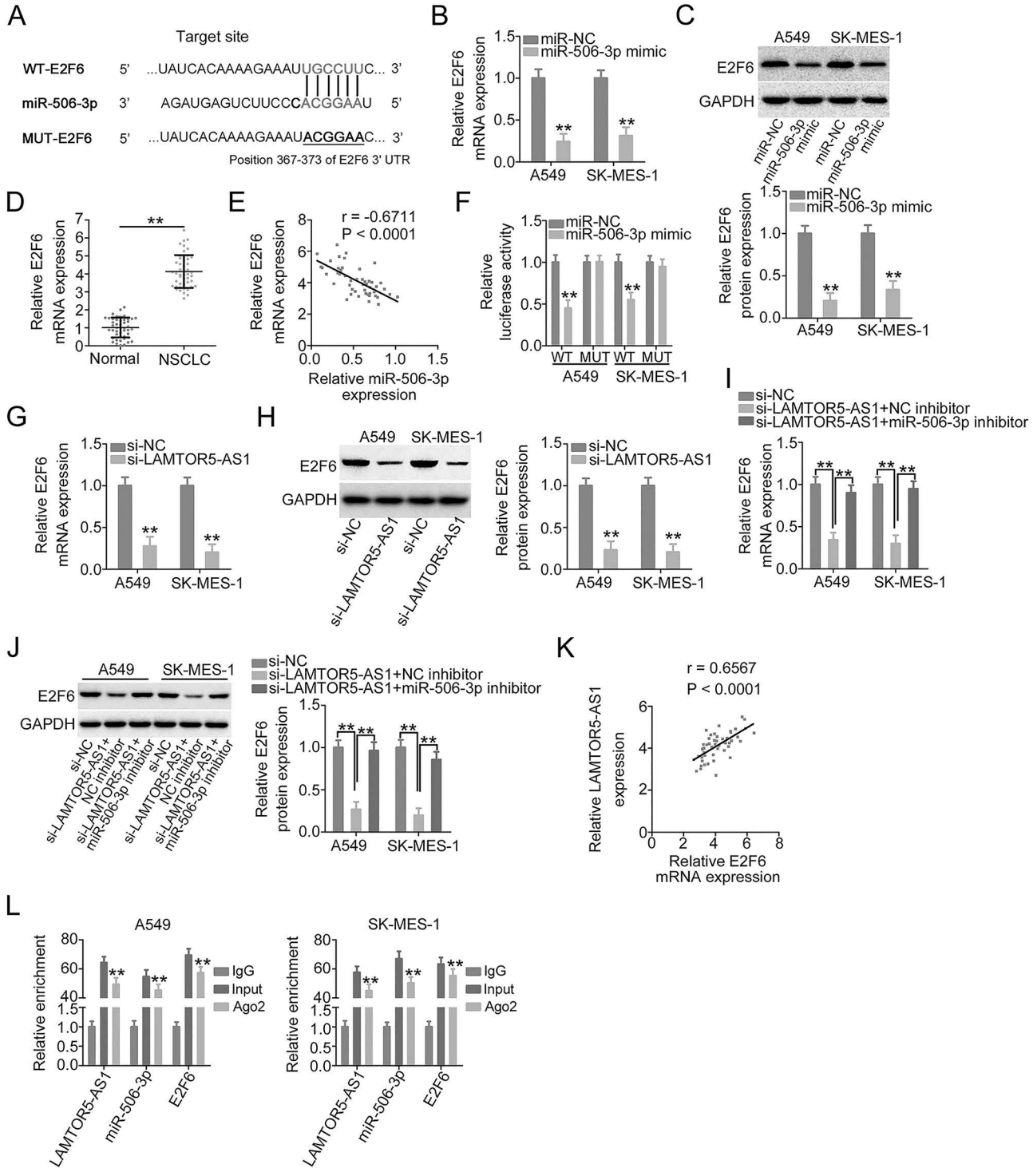

Figure 6. E2F6 is controlled by the LAMTOR5-AS1/miR-506-3p axis in NSCLC. (A) The WT and MUT binding sequences of miR-506-3p within the E2F6 3′-untranslated region (3′-UTR). (B, C) E2F6 expression was measured in miR-506-3p mimic-transfected NSCLC cells. (D) E2F6 mRNA levels in NSCLC tissues were determined via qRT-PCR. (E) The expression relationship between miR-506-3p and E2F6 in NSCLC tissues. (F) Luciferase activity was evaluated in miR-506-3p-overexpressing NSCLC cells after transfection with WT-E2F6 or MUT-E2F6. (G, H) Detection of E2F6 levels was conducted in NSCLC cells when LAMTOR5-AS1 was ablated. (I, J) LAMTOR5-AS1-silenced NSCLC cells were further probed with NC inhibitor or miR-506-3p inhibitor and subjected to assessment of E2F6 levels. (K) Expression correlation between LAMTOR5-AS1 and E2F6 in NSCLC tissues. (L) The enrichment of LAMTOR5-AS1, miR-506-3p, and E2F6 by Ago2 antibody was confirmed with a RIP assay. $^{**}p < 0.01$.

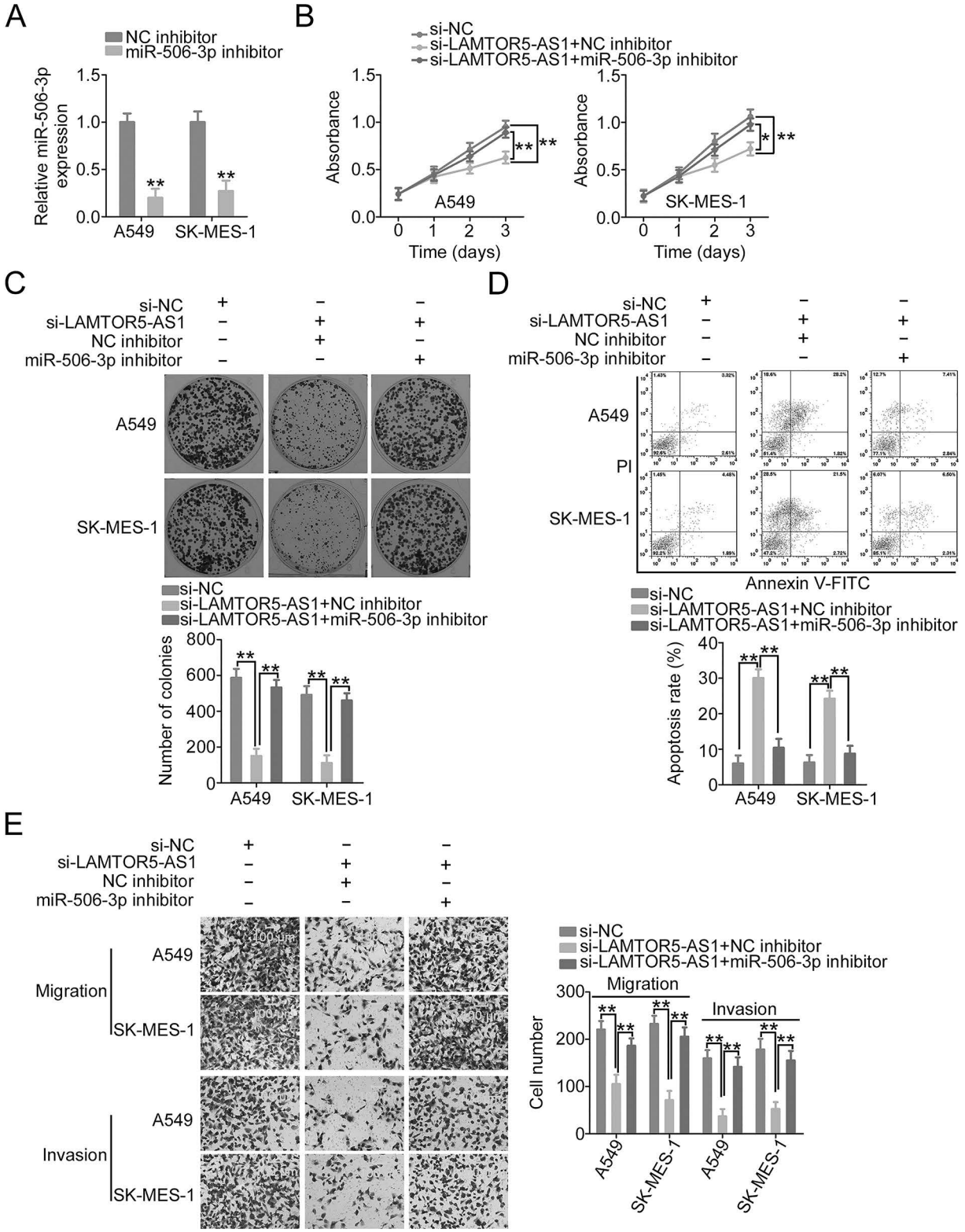

Figure 7. Inhibition of miR-506-3p abrogates the suppressive actions of si-LAMTOR5-AS1 in NSCLC. (A) The efficiency of the miR-506-3p inhibitor was determined by qRT-PCR. (B–D) NSCLC cells were transfected with si-NC, si-LAMTOR5-AS1+ NC inhibitor, or si-LAMTOR5-AS1+ miR-506-3p inhibitor. Cellular proliferation, colony formation, and apoptosis were assessed using CCK-8, colony formation, and flow cytometry assays. (E) Transwell experiments were performed to evaluate the motility of NSCLC cells treated as described above. *$p < 0.05$ and **$p < 0.01$.

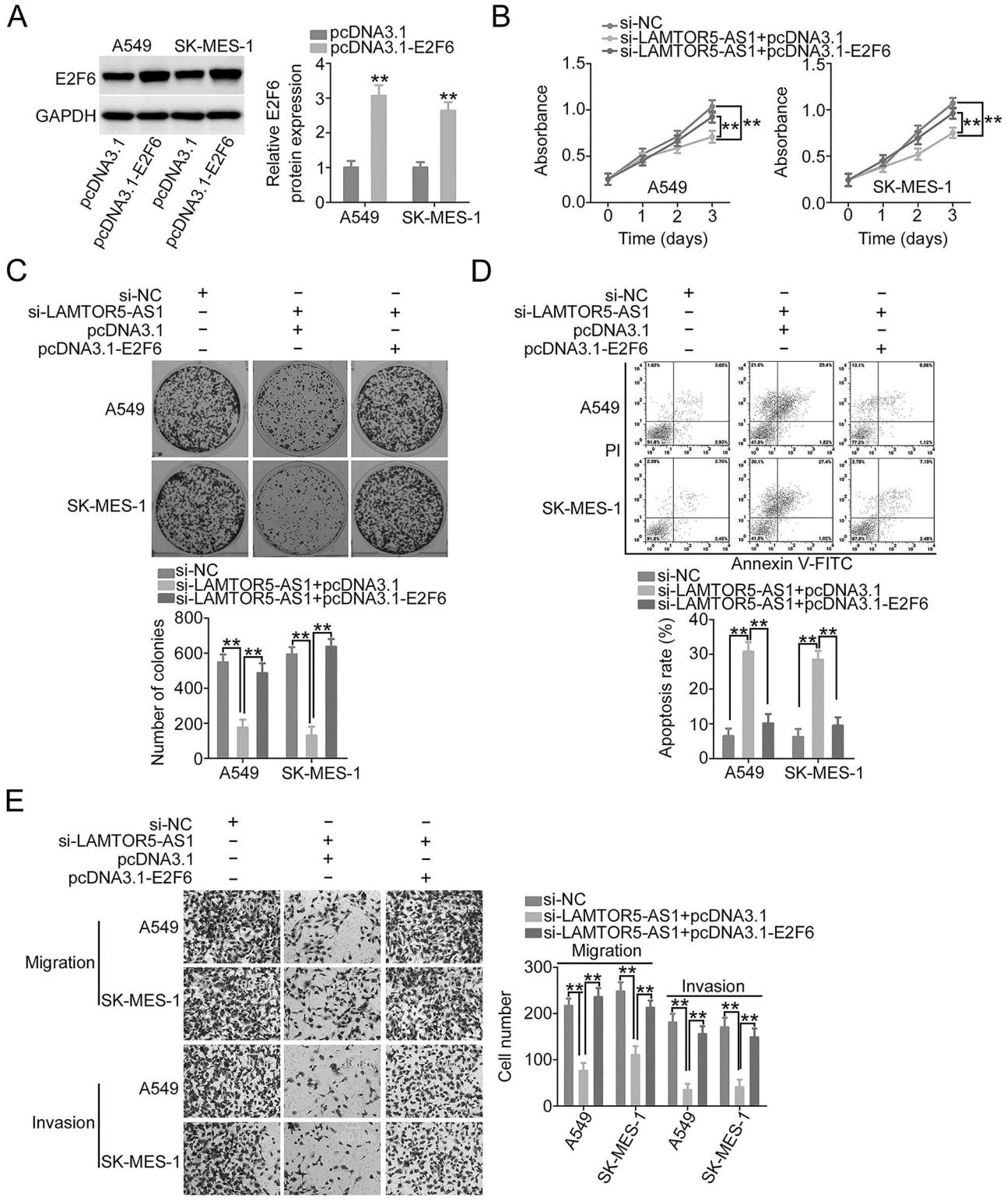

Figure 8. The tumor-inhibiting actions of si-LAMTOR5-AS1 in NSCLC are neutralized by E2F6 overexpression. (A) Successful transfection of pcDNA3.1-E2F6 was demonstrated by Western blotting. (B–D) pcDNA3.1-E2F6 or pcDNA3.1 alongside si-LAMTOR5-AS1 was transfected into NSCLC cells. CCK-8 assay, colony formation assay, and flow cytometry were implemented to assess cell proliferation, colony formation, and apoptosis, respectively. (E) NSCLC cells treated as described above were subjected to Transwell experiments for cell migration and invasion determination. $^{**}p < 0.01$.

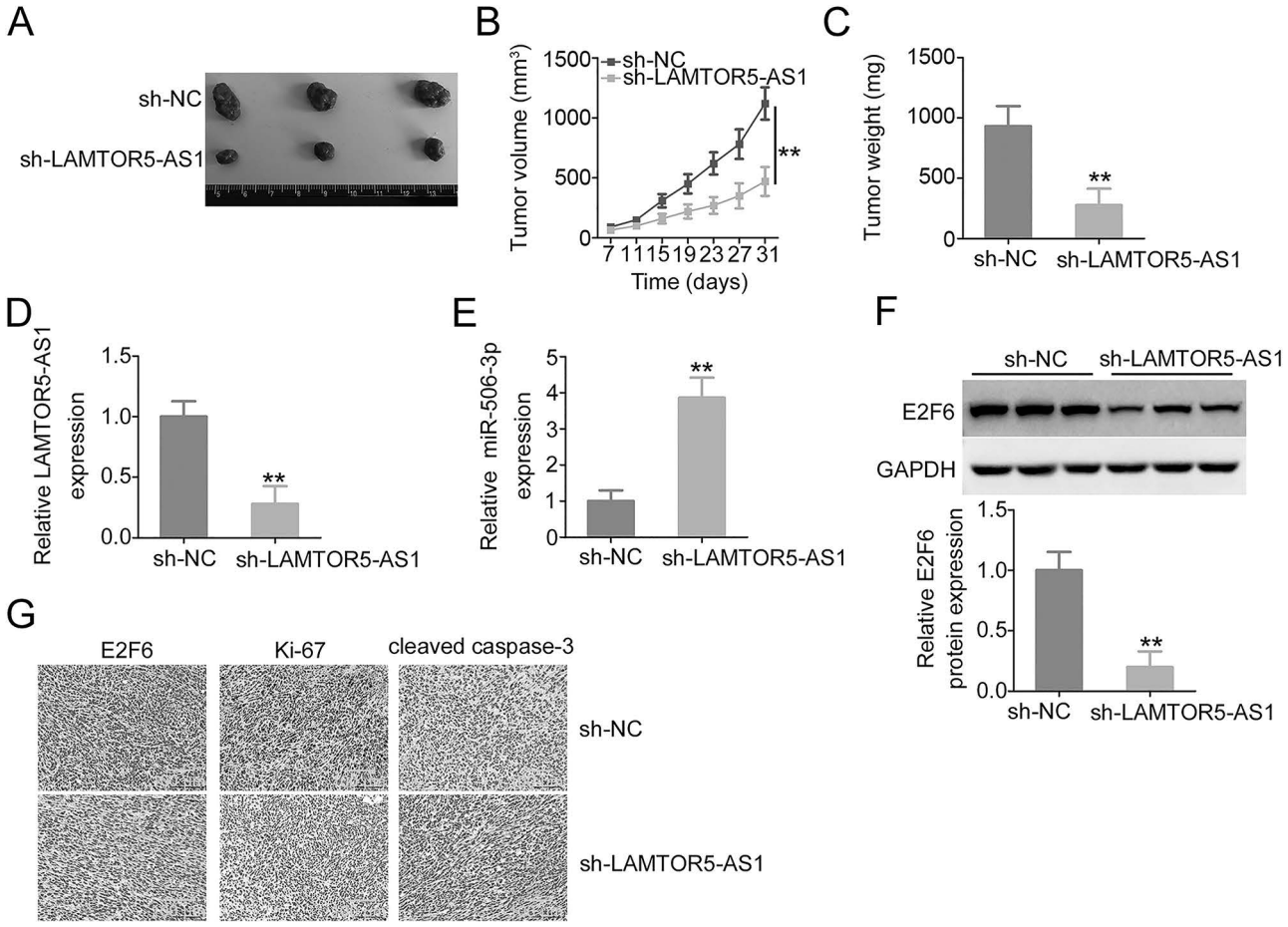

Figure 9. Knocking down LAMTOR5-AS1 represses tumor growth in vivo. (A) Images of the representative tumor xenografts. A total of six mice were used. Each group had three nude mice. (B) Tumor volume was recorded and applied to plot a growth curve. (C) The weight of tumor xenografts. (D–F) Levels of LAMTOR5-AS1, miR-506-3p, and E2F6 in tumors were determined. (G) Immunohistochemistry analysis of E2F6, Ki-67, and cleaved caspase-3 levels in tumor xenografts. $^{**}p < 0.01$.

was knocked down to assess the functional alterations in NSCLC cells in response to LAMTOR5-AS1 depletion.

LAMTOR5-AS1 has been affirmed to be a risk prediction and diagnostic biomarker of prostate cancer[21]. However, the expression and biological roles of LAMTOR5-AS1 in NSCLC are unclear. Herein, LAMTOR5-AS1 overexpression in NSCLC was verified in TCGA datasets and our own cohort and manifested an evident relationship with poor prognosis. Functionally, LAMTOR5-AS1 ablation led to repression of the proliferation, cloning, and metastasis abilities of NSCLC cells in vitro. We further observed an obvious increase in LAMTOR5-AS1-silenced NSCLC cell apoptosis. Additionally, the impact of LAMTOR5-AS1 downregulation on in vivo tumor growth was tested, and the inhibitory influence of LAMTOR5-AS1 depletion on NSCLC cell tumor growth was confirmed in vivo. All these observations reveal the importance of LAMTOR5-AS1 in NSCLC oncogenesis and progression.

The operating mode of lncRNAs is defined by their subcellular distribution[27]. In general, lncRNAs distributed in the cell nucleus affect transcriptional events, whereas cytoplasmic lncRNAs are implicated in post-transcriptional modulation[28]. The ceRNA theory has been gaining increasing interest in lncRNA research[29–31]. The theory connects the function of protein-coding mRNAs with that of miRNAs and lncRNAs[32]. lncRNAs serve as natural sponges for specific miRNAs, which in turn lowers the regulatory action of miRNAs on downstream target mRNAs.

In the current research, LAMTOR5-AS1 was discovered to be located mainly in the cytoplasmic fraction of NSCLC cells, indicating the posttranscriptional activity of this lncRNA. To unravel the molecular events downstream of LAMTOR5-AS1, bioinformatics prediction was implemented and indicated that an miR-506-3p binding site was present in LAMTOR5-AS1. In subsequent experiments, LAMTOR5-AS1 was found to

sponge miR-506-3p in NSCLC cells. Furthermore, E2F6, a downstream target of miR-506-3p, was under the control of LAMTOR5-AS1, which was realized by decoying miR-506-3p. In summary, miR-506-3p functions as a bridge between LAMTOR5-AS1 and E2F6, and together, they constitute a new ceRNA pathway in NSCLC, thus contributing to aggressive events.

miR-506-3p presents an aberrant expression pattern in many human cancers. For instance, a high level of miR-506-3p was confirmed in retinoblastoma[33] and pancreatic ductal adenocarcinoma[34], exerting pro-oncogenic actions. In contrast, osteosarcoma[35], papillary thyroid cancer[36], ovarian cancer[37], and nasopharyngeal carcinoma[38] weakly expressed miR-506-3p. In NSCLC, miR-506-3p was downregulated and exhibited a striking association with several aggressive clinicopathological characteristics and poor prognosis[39]. miR-506-3p was confirmed as a tumor-suppressing miRNA in NSCLC and is involved in malignant properties and gefitinib resistance[39,40]. In accordance with this, our data revealed a decreased level of miR-506-3p in NSCLC and uncovered its vital roles. More importantly, miR-506-3p directly targeted and lowered E2F6 expression in NSCLC cells. Rescue experiments verified that miR-506-3p suppression or E2F6 reintroduction was capable of remitting LAMTOR5-AS1 deficiency-triggered anticarcinogenic actions in NSCLC. Accordingly, the antineoplastic functions of LAMTOR5-AS1 silencing occurred through its ability to act as a ceRNA for miR-506-3p, consequently weakening the regulatory influences of the latter on E2F6 levels.

The current research contained two limitations. The regulatory effect of LAMTOR5-AS1 on metastasis in vivo was not explored. Furthermore, the related genes contributed to the influences of LAMTOR5-AS1 ablation on NSCLC cell growth, and metastasis should be analyzed. We will resolve the two limitations in the near future. More importantly, we will illuminate the downstream signaling pathway of LAMTOR5-AS1/miR-506-3p/E2F6 in NSCLC.

In summary, our study demonstrated the functions of LAMTOR5-AS1 for the first time and revealed that LAMTOR5-AS1 knockdown disrupted the malignancy of NSCLC by targeting the miR-506-3p/E2F6 axis. Certification of the LAMTOR5-AS1/miR-506-3p/E2F6 pathway may offer novel targets for NSCLC diagnosis and management.

ACKNOWLEDGMENTS: *The present study received approval from the Ethics Committee of The First People's Hospital of Yancheng. The experiments involving animals were implemented with approval from the Animal Ethics Committee of The First People's Hospital of Yancheng. Our current research was supported by Yancheng No.1 People's Hospital. This study was designed by Bo Chen and Guojie Chen. Guojie Chen, Kai Wang, Guoshu Li, Leidong Wang, and Yangyang Xiao performed all functional experiments. Bo Chen analyzed the data of the current research. Bo Chen and Guojie Chen wrote the manuscript. The authors declare no conflicts of interest.*

REFERENCES

1. Bray F, Ferlay J, Soerjomataram I, Siegel RL, Torre LA, Jemal A. 2020. Erratum: Global cancer statistics 2018: Globocan estimates of incidence and mortality worldwide for 36 cancers in 185 countries. CA Cancer J Clin. 70(4): 313.
2. Larsen JE, Minna JD. 2011. Molecular biology of lung cancer: Clinical implications. Clin Chest Med. 32(4):703–740.
3. Hirsch FR, Scagliotti GV, Mulshine JL, Kwon R, Curran WJ, Jr., Wu YL, Paz-Ares L. 2017. Lung cancer: Current therapies and new targeted treatments. Lancet 389(10066):299–311.
4. Bade BC, Dela Cruz CS. 2020. Lung cancer 2020: Epidemiology, etiology, and prevention. Clin Chest Med. 41(1):1–24.
5. Nishimura T, Nakamura H, Vegvari A, Marko-Varga G, Furuya N, Saji H. 2019. Current status of clinical proteogenomics in lung cancer. Expert Rev Proteomics 16(9):761–772.
6. Zhao L, Liu C, Xie G, Wu F, Hu C. 2020. Multiple primary lung cancers: A new challenge in the era of precision medicine. Cancer Manag Res. 12:10361–10374.
7. Wu S, Pan Y, Mao Y, Chen Y, He Y. 2021. Current progress and mechanisms of bone metastasis in lung cancer: A narrative review. Transl Lung Cancer Res. 10(1):439–451.
8. Kopp F, Mendell JT. 2018. Functional classification and experimental dissection of long noncoding RNAs. Cell. 172(3):393–407.
9. Li H, Ma SQ, Huang J, Chen XP, Zhou HH. 2017. Roles of long noncoding RNAs in colorectal cancer metastasis. Oncotarget. 8(24):39859–39876.
10. Abolghasemi M, Tehrani SS, Yousefi T, Karimian A, Mahmoodpoor A, Ghamari A, Jadidi-Niaragh F, Yousefi M, Kafil HS, Bastami M, Edalati M, Eyvazi S, Naghizadeh M, Targhazeh N, Mihanfar A, Yousefi B, Safa A, Majidinia M, Rameshknia V. 2020. Critical roles of long noncoding RNAs in breast cancer. J Cell Physiol. 235(6):5059–5071.
11. Chen W, Liu S, Wang F. 2021. Potential impact and mechanism of long non-coding RNAs on cancer and associated T cells. J Cancer 12(16):4873–4882.
12. La Montagna M, Ginn L, Garofalo M. 2021. Mechanisms of drug resistance mediated by long non-coding RNAs in non-small-cell lung cancer. Cancer Gene Ther. 28(3–4):175–187.
13. Shen D, Li J, Tao K, Jiang Y. 2021. Long non-coding RNA MCM3AP antisense RNA 1 promotes non-small cell lung cancer progression through targeting microRNA-195-5p. Bioengineered 12(1):3525–3538.
14. Chen Z, Lei T, Chen X, Gu J, Huang J, Lu B, Wang Z. 2020. Long non-coding RNA in lung cancer. Clin Chim Acta 504:190–200.
15. Lagos-Quintana M, Rauhut R, Lendeckel W, Tuschl T. 2001. Identification of novel genes coding for small expressed RNAs. Science 294(5543):853–858.
16. Bartel DP. 2004. MicroRNAs: Genomics, biogenesis, mechanism, and function. Cell 116(2):281–297.
17. Liu YR, Wang PY, Xie N, Xie SY. 2020. MicroRNAs as therapeutic targets for anticancer drugs in lung cancer therapy. Anticancer Agents Med Chem. 20(16):1883–1894.
18. Shangguan WJ, Liu HT, Que ZJ, Qian FF, Liu LS, Tian JH. 2019. Tob1-as1 suppresses non-small cell lung cancer

cell migration and invasion through a ceRNA network. Exp Ther Med. 18(6):4249–4258.
19. Yang Y, Li S, Cao J, Li Y, Hu H, Wu Z. 2019. RRM2 regulated by LINC00667/miR-143-3p signal is responsible for non-small cell lung cancer cell progression. Onco Targets Ther. 12:9927–9939.
20. Chen X, Wang Z, Tong F, Dong X, Wu G, Zhang R. 2020. LncRNA UCA1 promotes gefitinib resistance as a ceRNA to target FOSL2 by sponging miR-143 in non-small cell lung cancer. Mol Ther Nucleic Acids 19:643–653.
21. Li Z, Zheng J, Xia Q, He X, Bao J, Chen Z, Katayama H, Yu D, Zhang X, Xu J, Zhu T, Wang J. 2020. Identification of specific long non-coding ribonucleic acid signatures and regulatory networks in prostate cancer in fine-needle aspiration biopsies. Front Genet. 11:62.
22. Livak KJ, Schmittgen TD. 2001. Analysis of relative gene expression data using real-time quantitative pcr and the 2(-delta delta c(t)) method. Methods 25(4):402–408.
23. Wang L, Ma L, Xu F, Zhai W, Dong S, Yin L, Liu J, Yu Z. 2018. Role of long non-coding RNA in drug resistance in non-small cell lung cancer. Thorac Cancer 9(7):761–768.
24. Li L, Zhang X, Liu Q, Yin H, Diao Y, Zhang Z, Wang Y, Gao Y, Ren X, Li J, Cui D, Lu Y, Liu H. 2019. Emerging role of HOX genes and their related long noncoding RNAs in lung cancer. Crit Rev Oncol Hematol. 139:1–6.
25. Lin S, Zhen Y, Guan Y, Yi H. 2020. Roles of Wnt/β-catenin signaling pathway regulatory long non-coding RNAs in the pathogenesis of non-small cell lung cancer. Cancer Manag Res. 12:4181–4191.
26. Castillo J, Stueve TR, Marconett CN. 2017. Intersecting transcriptomic profiling technologies and long non-coding RNA function in lung adenocarcinoma: Discovery, mechanisms, and therapeutic applications. Oncotarget. 8(46):81538–81557.
27. Carlevaro-Fita J, Johnson R. 2019. Global positioning system: Understanding long noncoding RNAs through subcellular localization. Mol Cell 73(5):869–883.
28. Statello L, Guo CJ, Chen LL, Huarte M. 2021. Gene regulation by long non-coding rnas and its biological functions. Nat Rev Mol Cell Biol. 22(2):96–118.
29. Li J, Xu X, Zhang D, Lv H, Lei X. 2021. LncRNA LHFPL3-AS1 promotes oral squamous cell carcinoma growth and cisplatin resistance through targeting miR-362-5p/CHSY1 pathway. Onco Targets Ther. 14:2293–2300.
30. Niu ZS, Wang WH, Dong XN, Tian LM. 2020. Role of long noncoding RNA-mediated competing endogenous RNA regulatory network in hepatocellular carcinoma. World J Gastroenterol. 26(29):4240–4260.
31. Ye Y, Shen A, Liu A. 2019. Long non-coding RNA h19 and cancer: A competing endogenous RNA. Bull Cancer 106(12):1152–1159.
32. Wu Y, Qian Z. 2019. Long non-coding RNAs (lncRNAs) and microRNAs regulatory pathways in the tumorigenesis and pathogenesis of glioma. Discov Med. 28(153): 129–138.
33. Song Z, Wang H, Zong F, Zhu C, Tao Y. 2019. MicroRNA 506 regulates apoptosis in retinoblastoma cells by targeting sirtuin 1. Cancer Manag Res. 11:8419–8429.
34. Cheng RF, Wang J, Zhang JY, Sun L, Zhao YR, Qiu ZQ, Sun BC, Sun Y. 2016. MicroRNA-506 is up-regulated in the development of pancreatic ductal adenocarcinoma and is associated with attenuated disease progression. Chin J Cancer. 35(1):64.
35. Ding L, Sun R, Yan Q, Wang C, Han X, Cui Y, Li R, Liu J. 2021. MiR-506 exerts antineoplastic effects on osteosarcoma cells via inhibition of the Skp2 oncoprotein. Aging (Albany NY) 13(5):6724–6739.
36. Zhu J, Zhang Q, Jin XY, Cai JB, Chen X, Shi WB, Pang WY, Guo GL, Yang LJ. 2019. MiR-506 suppresses papillary thyroid carcinoma cell proliferation and metastasis via targeting IL17RD. Eur Rev Med Pharmacol Sci. 23(7):2856–2862.
37. Xia XY, Yu YJ, Ye F, Peng GY, Li YJ, Zhou XM. 2020. MicroRNA-506-3p inhibits proliferation and promotes apoptosis in ovarian cancer cell via targeting SIRT1/AKT/FOXO3a signaling pathway. Neoplasma 67(2):344–353.
38. Fan DC, Zhao YR, Qi H, Hou JX, Zhang TH. 2020. MiRNA-506 presents multiple tumor suppressor activities by targeting EZH2 in nasopharyngeal carcinoma. Auris Nasus Larynx 47(4):632–642.
39. Guo S, Yang P, Jiang X, Li X, Wang Y, Zhang X, Sun B, Zhang Y, Jia Y. 2017. Genetic and epigenetic silencing of mircorna-506-3p enhances cotl1 oncogene expression to foster non-small lung cancer progression. Oncotarget 8(1):644–657.
40. Zhu J, Tao L, Jin L. 2019. MicroRNA5063p reverses gefitinib resistance in nonsmall cell lung cancer by targeting yesassociated protein 1. Mol Med Rep. 19(2):1331–1339.